

Applications of Cluster Perturbation Theory Using Quantum Monte Carlo Data

Fei Lin, Erik S. Sørensen, Catherine Kallin and A. John Berlinsky

Department of Physics and Astronomy, McMaster University, Hamilton, Ontario, Canada L8S 4M1

Abstract

*We study cluster perturbation theory [Phys. Rev. Lett. **84**, 522 (2000)] when auxiliary field quantum Monte Carlo method is used for solving the cluster hamiltonian. As a case study, we calculate the spectral functions of the Hubbard model in one and two dimensions and compare our results for the spectral functions to results obtained using exact diagonalization to solve the cluster hamiltonian. The main advantage of using quantum Monte Carlo results as a starting point is that the initial cluster size can be taken to be considerably larger and hence potentially capture more of the relevant physics. The drawback is that quantum Monte Carlo methods yield results at imaginary times with stochastic errors.*

1 Introduction

In the field of strongly-correlated systems (such as the high-temperature superconductors), it is usually useful to study the single-particle excitation spectrum. Experimentally, it can be obtained through the ARPES technique for some systems [3]; while theoretically, it can be calculated by exact diagonalization (ED) or quantum Monte Carlo (QMC) method for some finite lattice models, such as the Hubbard model, which describes a lattice system of strongly-interacting electrons and which is believed by some Physicists to capture the Physics of the high-temperature superconductors.

Since these calculations are for a finite system, it is desirable to extend the calculations to the infinite lattice systems for a better comparison between the experiments and the theoretical calculations. Cluster perturbation theory (CPT) as proposed by Sénéchal *et al.* [10, 11] is one of these extensions, and has turned out to be an accurate and economical technique for calculating the spectral functions of the Hubbard model in one- and two-dimensional (1D and 2D) lattice systems. The method starts by dividing the infinite lattice system into a periodic array of clusters. The Hubbard model inside a cluster is then solved by ED, and the hopping matrix between two neighboring clusters is treated

as a perturbation. The cluster Green's functions from ED are then used to perturbatively construct the Green's functions of the infinite lattice. The method is economical in that one usually only diagonalizes a small cluster (typically less than 14 sites for the Hubbard model), and the infinite lattice Green's function with an arbitrary momentum \mathbf{k} can then be constructed with a very small computational overhead. The computationally limiting step is therefore the exact diagonalization of the cluster which effectively limits its size to less than 20 sites or so for the Hubbard model. (The computer memory requirement grows exponentially with increasing cluster sizes.) On the other hand many materials, such as molecular solids, display a "natural" cluster size (the molecule) which may be significantly beyond what can be treated with exact diagonalization techniques and it therefore becomes of great interest to study the accuracy of cluster perturbation theory when the cluster itself is treated with approximate techniques.

In this paper we study the accuracy of the CPT method [10, 11] when auxiliary field quantum Monte Carlo (AFQMC) methods [6, 7, 12] are used to solve the cluster Hamiltonian. To distinguish between these two methods, we call the usual CPT method using exact diagonalization methods to solve the cluster hamiltonian EDCPT and analogously the present method QMCPT. The advantage of QMCPT is that we can deal with clusters as large as 60 sites (results will be presented elsewhere) as long as the sign problem [6], which is the appearance of negative probabilities in the QMC simulations, is not too severe. However, AFQMC yields *imaginary* time Green's functions with stochastic errors. In order to use such Green's functions as input to the zero temperature cluster perturbation theory formalism an analytic continuation to real times (frequency) has to be performed, a notoriously difficult step. Hence, it is not obvious that this approach will yield reliable results. Fortunately, as we show in the following, if high precision numerical data are available for the imaginary time Green's functions an analytical continuation using maximum entropy methods of the AFQMC data yield results that are in quite good agreement with EDCPT for the same cluster size.

In the next section we briefly introduce the EDCPT method. This is followed by the introduction of AFQMC

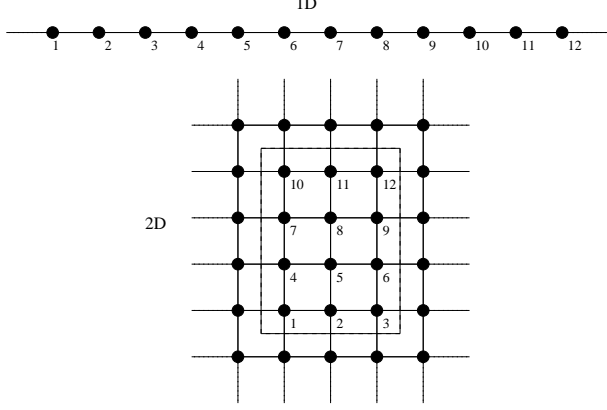


Figure 1. 1D and 2D clusters for the CPT calculations. In 1D a cluster of 12 sites is used in the paper. A 3×4 cluster is drawn for the 2D square lattice.

and QMCPT, describing details in the calculation. Spectral functions of the 1D and 2D Hubbard Hamiltonians are then presented and compared to those obtained using EDCPT.

2 Model

The model Hamiltonian we consider is given by

$$H = H_0 + V, \quad (1)$$

$$H_0 = \sum_I H_0^I, \quad (2)$$

where

$$H_0^I = -t \sum_{\langle ij \rangle \sigma} (c_{i\sigma}^\dagger c_{j\sigma} + h.c.) + U \sum_i n_{i\uparrow} n_{i\downarrow} \quad (3)$$

is the Hubbard model inside the I 'th cluster, and

$$V = -t' \sum_{\langle Ii, Jj \rangle \sigma} (c_{Ii\sigma}^\dagger c_{Jj\sigma} + h.c.) \quad (4)$$

is the hopping terms between two nearest neighbor (NN) sites i and j in two NN clusters I and J , respectively. Here the operator notations are standard for the usual Hubbard model, i.e., $c_{i\sigma}^\dagger$ ($c_{i\sigma}$) is the electron creation (annihilation) operator for spin σ , and $n_{i\sigma}$ is the electron number operator for site i with spin σ . Inside the cluster U is the on-site Coulomb interaction energy, and t is the hopping integral between two NN sites. When $t' = t$, we recover the standard Hubbard model. In the following calculations t is used as the energy unit.

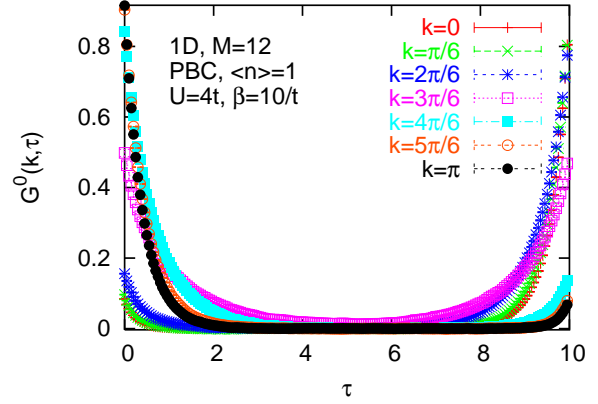


Figure 2. Evolution of cluster Green's function with imaginary time τ in QMC simulation. We see that enough amount of data has made the error bars very small, which is essential in MEM [8].

3 EDCPT Formalism

To compare EDCPT with QMCPT, we will briefly describe the calculational steps of EDCPT for the Hubbard model. EDCPT first uses the Lanczos algorithm [5], which is an efficient method for obtaining several lowest eigen values of sparse matrices, to diagonalize the Hubbard Hamiltonian H_0^I of a cluster for its ground state energy E_0 and the corresponding eigen state $|\Psi\rangle$. The single-particle Green's function is then given by

$$G_{ij}^0(\omega) = G_{ij}^e(\omega) + G_{ij}^h(\omega), \quad (5)$$

$$G_{ij}^e(\omega) = \langle \Psi | c_i \frac{1}{\omega + i\eta + E_0 - H_0^I} c_j^\dagger | \Psi \rangle, \quad (6)$$

$$G_{ij}^h(\omega) = \langle \Psi | c_i^\dagger \frac{1}{\omega + i\eta - E_0 + H_0^I} c_j | \Psi \rangle, \quad (7)$$

where e and h represent respectively the electron and hole part of the green's function, and η is a small positive parameter to give the Lorentzian broadening of the delta functions. The calculation of these cluster Green's functions is standard, and can be found in the literature (e.g., Ref. [9]).

With these Green's functions $G_{ij}^0(\omega)$, the Green's functions for the superlattice $G(\mathbf{K}, \omega)$ is constructed through the strong coupling perturbation [10, 11]:

$$G_{ij}(\mathbf{K}, \omega) = \left(\frac{G_{ij}^0(\omega)}{1 - V(\mathbf{K})G^0(\omega)} \right)_{ij}, \quad (8)$$

where \mathbf{K} is superlattice's momentum vector, and $V(\mathbf{K})$ is the Fourier transform of Eq. (4). $V(\mathbf{K})$ is given by

$$V_{ij}(\mathbf{K}) = \sum_{\mathbf{R}} V_{ij}^0 \mathbf{R} e^{i\mathbf{K} \cdot \mathbf{R}}, \quad (9)$$

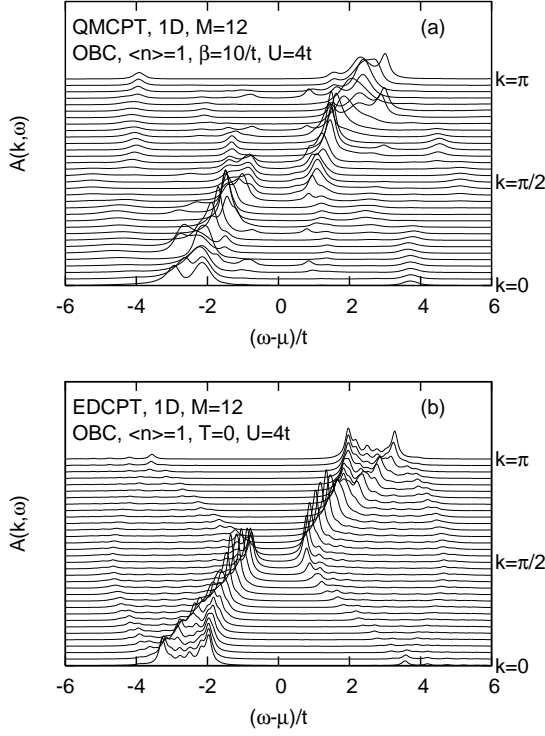


Figure 3. Single particle spectral functions of the 1D Hubbard model from (a) QMCPT and (b) EDCPT with open boundary conditions. Both methods produce roughly the same single-particle excitation energies $(\omega - \mu)/t$ and energy gap value, although the spectral height is different at some energy values. See text for the reason.

where \mathbf{R} represents position of the cluster in the superlattice. A residual Fourier transform is performed to construct the lattice Green's functions in terms of the \mathbf{k} vectors of the original lattice

$$G_{\text{CPT}}(\mathbf{k}, \omega) = \frac{1}{M} \sum_{i,j=1}^M G_{ij}(\mathbf{k}, \omega) e^{-i\mathbf{k} \cdot (\mathbf{r}_i - \mathbf{r}_j)}, \quad (10)$$

where M is the number of lattice sites in one cluster. The spectral function of the infinite lattice is then given by

$$A(\mathbf{k}, \omega) = -\frac{1}{\pi} \lim_{\eta \rightarrow 0^+} \text{Im} G_{\text{CPT}}(\mathbf{k}, \omega). \quad (11)$$

4 QMCPT Formalism

In QMCPT the imaginary-time cluster Green's functions $G^0(\mathbf{k}, \tau)$ are calculated using the auxiliary field QMC tech-

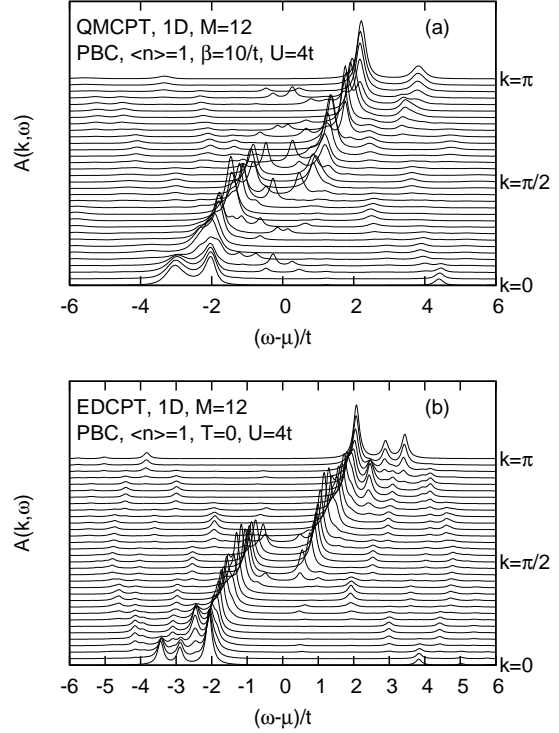


Figure 4. Comparison of single particle spectral functions of a 1D Hubbard model from (a) QMCPT and (b) EDCPT with periodic boundary conditions. Both methods give roughly the same single-particle excitation energies at most energy values, but the spurious excitations inside the energy gap shows that QMCPT with periodic boundary conditions is inaccurate.

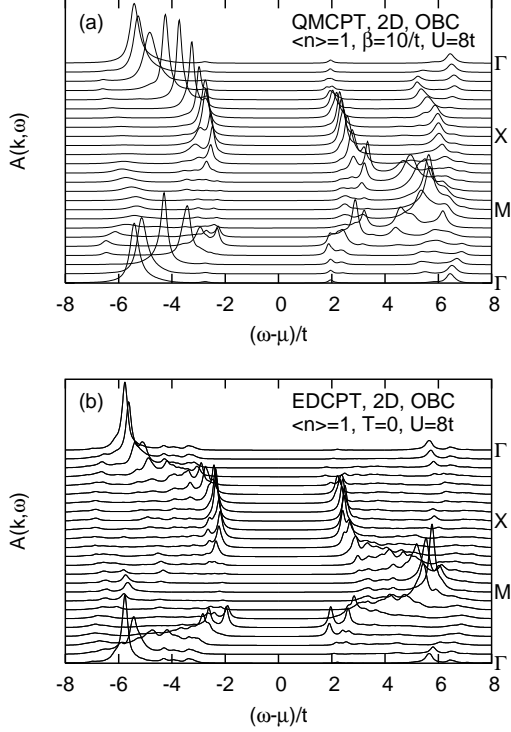


Figure 5. Single particle spectral functions of a 2D Hubbard model from (a) QMCPT and (b) EDCPT with open boundary conditions. The cluster is of dimension 3×4 . Both methods predict the same single-particle excitation energies and energy gap, though at some energy values the spectral height is different. See text for the reason.

nique [6, 7, 12]. They are then analytically continued to extract the real frequency spectral functions $A^0(\mathbf{k}, \omega)$ through the Maximum Entropy method (MEM) [8]:

$$G^0(\mathbf{k}, \tau) = \int d\omega \frac{e^{-\tau\omega} A^0(\mathbf{k}, \omega)}{1 + e^{-\beta\omega}}, \quad (12)$$

where $\beta = 1/k_B T$ is the inverse temperature in the QMC simulation, and τ is the imaginary time. The above integral in Eq. (12) is discretized with a small $\Delta\omega$ and summed over a set of $A^0(\mathbf{k}, \omega)$ values. A smaller $\Delta\omega$ produces a smoother image for $A^0(\mathbf{k}, \omega)$, but different $\Delta\omega$ usually gives results in agreement with each other. We refer the interested readers to Ref. [8] for the details of MEM. The resulting $A^0(\mathbf{k}, \omega)$ can be used to construct the real frequency cluster Green's functions via [4]

$$G^0(\mathbf{k}, \omega) = \int d\omega' \frac{A^0(\mathbf{k}, \omega')}{\omega + i\eta - \omega'}. \quad (13)$$

After a cluster Fourier transform from the \mathbf{k} vectors to cluster i, j indices, and again following Eqs. (8), (9), (10) and (11), we can evaluate the spectral functions $A(\mathbf{k}, \omega)$ for the infinite lattice.

Next we discuss in detail the calculation of space-time Green's functions with QMC simulations. Since we are considering only the cluster Hamiltonian, we can neglect Eq. (4) and write Eq. (3) as

$$H_0^I = T + W, \quad (14)$$

where

$$T = -t \sum_{\langle ij \rangle \sigma} (c_{i\sigma}^\dagger c_{j\sigma} + h.c.) \quad (15)$$

and

$$W = U \sum_i n_{i\uparrow} n_{i\downarrow} \quad (16)$$

representing, respectively, the kinetic and potential energies of the cluster.

The partition function is then given by

$$\begin{aligned} Z &= \text{Tr} e^{-\beta(T+W)} \\ &= \text{Tr} \prod_{i=1}^L e^{-\Delta\tau(T+W)}, \end{aligned} \quad (17)$$

where $\beta = \Delta\tau L$, and L is the number of time slices in the imaginary time direction. After tracing out the fermionic operators, we get

$$\begin{aligned} Z &= \sum_{\{\sigma\}} \prod_{\alpha} \det[1 + B_L(\alpha) B_{L-1}(\alpha) \cdots B_1(\alpha)] \\ &= \sum_{\{\sigma\}} \det O(\{\sigma\}, \mu)_{\uparrow} \det O(\{\sigma\}, \mu)_{\downarrow}. \end{aligned} \quad (18)$$

The B_l matrices are defined as

$$B_l(\alpha) = e^{-\Delta\tau T} e^{W^\alpha(l)}, \quad (19)$$

$$(T)_{ij} = \begin{cases} -t_{ij} & \text{for } i, j \text{ NN,} \\ 0 & \text{otherwise,} \end{cases} \quad (20)$$

$$W_{ij}^\alpha(l) = \delta_{ij}[\lambda\alpha\sigma_i(l) + \mu\Delta\tau], \quad (21)$$

where μ is chemical potential, $\tanh^2(\lambda/2) = \tanh(\Delta\tau U/4)$, $\sigma_i(l) = \pm 1$ is the auxiliary Ising spin coupled with the electrons at lattice site i and time $\tau = (l-1)\Delta\tau$, and $\alpha = \pm 1$ corresponds to \uparrow or \downarrow in Eq. (18).

In calculating the space-time Green's functions, we form a matrix of dimension $ML \times ML$ after a complete sweep over the M cluster sites and L time slices, the inverse of which gives the desired cluster Green's functions [1, 7]

$$\begin{pmatrix} 1 & 0 & \cdot & 0 & B_1 \\ -B_2 & 1 & 0 & \cdot & 0 \\ 0 & -B_3 & 1 & \cdot & 0 \\ \cdot & 0 & -B_4 & \cdot & \cdot \\ \cdot & \cdot & 0 & \cdot & \cdot \\ \cdot & \cdot & \cdot & \cdot & 0 \\ 0 & \cdot & 0 & -B_L & 1 \end{pmatrix}^{-1} = \begin{pmatrix} G^0(1,1) & G^0(1,2) & \cdot & \cdot & G^0(1,L) \\ G^0(2,1) & G^0(2,2) & \cdot & \cdot & G^0(2,L) \\ \cdot & \cdot & \cdot & \cdot & \cdot \\ G^0(L,1) & G^0(L,2) & \cdot & \cdot & G^0(L,L) \end{pmatrix},$$

where, for $l_1 > l_2$,

$$\begin{aligned} G_{ij}^0(l_1, l_2) &= \langle c_i(l_1) c_j^\dagger(l_2) \rangle \\ &= [B_{l_1} B_{l_1-1} \cdots B_{l_2+1} (1 + \\ &\quad B_{l_2} \cdots B_1 B_L \cdots B_{l_1+1})^{-1}]_{ij}. \end{aligned} \quad (22)$$

After a Fourier transform of the above Green's functions, we have $G_{\mathbf{k}}^0(l, 1) = G^0(\mathbf{k}, \tau)$, where $\tau = (l-1)\Delta\tau$ with $(1 \leq l \leq L)$. They are the input for the MEM algorithm in Eq. (12). Note that in the above definition of finite temperature Green's functions in Eq. (22) we used the same symbol as that for zero temperature in Eq. (5), since there is no difference in the application of the CPT method in these two cases.

5 Results

5.1 1D Case

In this section we will present QMCPT results on the 1D and 2D Hubbard models. See Fig. 1 for the division of the 1D and 2D lattices into clusters and the geometry of the respective clusters. We choose 12-site clusters in both 1D and 2D cases, so that we can compare the results with those

available in the literature. The intra-cluster hopping integral t is used as the energy unit, and the on-site Coulomb interaction $U = 4t$ or $U = 8t$. The inter-cluster hopping integral t' will be set to t , too. In QMC the inverse temperature is $\beta = 10/t$, which will produce results close to the ground state. The Lorentzian broadening parameter is $\eta = 0.1t$, which is of the same order of the QMC temperature.

In QMC simulations we discretize the imaginary time $\beta = 10/t$ into 200 slices, i.e., $\Delta\tau = 0.05/t$ to make the Trotter error smaller than the statistical ones. The 12-site Hubbard ring assumes either open boundary conditions (OBC) or periodic boundary conditions (PBC). One thousand complete sweeps over the space-time lattice are performed to warm up the system. For each boundary case, we collect 51,000 sets of space-time Green's functions, each 100 sets of which are averaged as 1 bin (total 510 bins) for the subsequent MEM analysis. A typical $G^0(\mathbf{k}, \tau)$ versus τ is shown in Fig. 2. For generating a smooth figure for $A^0(\mathbf{k}, \omega)$, the discretization of the real frequency is set at $\Delta\omega = 0.025t$ in MEM. Note that a smaller $\Delta\omega$ does not change the resultant figure except for making the figure smoother with longer computation times. Fig. 3 compares the QMCPT result with the EDCPT result for a 1D Hubbard chain constructed from the 12-site cluster with open boundary conditions. We find that QMCPT result agree very well with the EDCPT one. They both have a Hubbard gap opening at $\omega - \mu = 0$ and the same positions of spectral peaks, although the peak heights are different in some positions. Hence, a precise determination of the quasi-particle weights is probably not feasible with QMCPT. We expect this to happen, because MEM always broadens the sharp peaks or blurs the fine details of the exact results. In spite of this problem, QMCPT still produces spectral functions that satisfy the usual sum rules [4].

There has been a suggestion of using periodic boundary condition (PBC) in the clusters [2], which, in ED, can greatly reduce the dimension of the Hilbert space through the translational symmetry. These additional hopping terms are then subtracted from the perturbation V during the construction of the superlattice Green's functions. Comparison of the EDCPT results with open and periodic boundary conditions are made in Ref. [11], where both results agree in the sense that a Hubbard gap opens at half filling for both cases. Here we repeat the same calculations in the same systems with both QMCPT and EDCPT. The results are shown in both Fig. 3 and Fig. 4. We find that QMCPT calculations with periodic boundary conditions produce spurious single particle peaks around $\omega - \mu = 0$. Therefore, in what follows we use open boundary conditions in the QMCPT calculations.

5.2 2D Case

In the 2D Hubbard system, we choose a cluster of $M_x M_y = 3 \times 4$ (see Fig. 1) with open boundary conditions for QMC simulation. We have collected 71,000 sets of space-time Green's functions, which are averaged to yield 710 bins for MEM analysis. We find that in this $U = 8t$ case less sets of data makes the MEM analysis difficult [8]. The QMCPT result together with the EDCPT result are shown in Fig. 5, where the \mathbf{k} vector scan is along $\Gamma - M - X - \Gamma$ (Please see the figure illustration of this momentum space scan in Ref. [10]). We see that the QMCPT produces results close to those of EDCPT. (See also Ref. [10].) The main peaks found in EDCPT are all preserved in the QMCPT calculation, which again shows that we can safely use QMCPT for the lattice spectral function calculations (in that QMCPT predicts the correct single-particle excitation energies and energy gaps though with different spectral heights from EDCPT at some energy values). This is again because of the broadening of sharp peaks and the blurring of fine details in the MEM analysis.

6 Conclusions

In summary, we have presented our first effort in applying CPT method using AFQMC to solve the cluster hamiltonian. At low temperatures our QMC and QMCPT results agree very well with those from EDCPT [10, 11]. Compared with EDCPT, QMCPT works at finite and very low temperatures, and the cluster sizes can be much larger. We expect QMCPT to be a useful tool in calculating the spectral functions in not only the 1D and 2D lattices but also some molecular solids, e.g., fullerene materials, where each molecule naturally defines a cluster, and ED of Hubbard model is not possible for molecules with more than 20 sites.

Acknowledgements

This project was supported by the Natural Sciences and Engineering Research Council (NSERC) of Canada, the Canadian Institute for Advanced Research (CIAR), and the Canadian Foundation for Innovation (CFI). All the calculations were carried out at SHARCNET supercomputing facilities at McMaster University.

References

- [1] F. F. Assaad. *NIC series*, 10:99, 2002.
- [2] C. Dahnken, E. Arrigoni, and W. Hanke. *J. Low Temp. Phys.*, 126:949, 2002.
- [3] A. Damasceli, Z. Hussain, and Z. Shen. *Rev. Mod. Phys.*, 75:473, 2003.
- [4] A. L. Fetter and J. D. Walecka. *Quantum Theory of Many-Particle Systems*. Dover Publications, Mineola, New York, 2003.
- [5] G. Golub and C. V. Loan. *Matrix Computations*. The Johns Hopkins University Press, Baltimore and London, 1989.
- [6] J. E. Hirsch. *Phys. Rev. B*, 31:4403, 1985.
- [7] J. E. Hirsch. *Phys. Rev. B*, 38:R12023, 1988.
- [8] M. Jarrell and J. E. Gubernatis. *Phys. Rep.*, 269:133, 1996.
- [9] H. Q. Lin and J. E. Gubernatis. *Comput. Phys.*, 7:400, 1993.
- [10] D. Sénéchal, D. Perez, and M. Pioro-Ladrière. *Phys. Rev. Lett.*, 84:522, 2000.
- [11] D. Sénéchal, D. Perez, and D. Plouffe. *Phys. Rev. B*, 66:075129, 2002.
- [12] S. R. White, D. J. Scalapino, R. L. Sugar, E. Y. Loh, J. E. Gubernatis, and R. T. Scalettar. *Phys. Rev. B*, 40:506, 1989.